JOURNAL OF GEOPHYSICAL RESEARCH, VOL. 105, NO. A11, PAGES 25,171–25,183, NOVEMBER 1, 2000

Two-dimensional hybrid simulation of the dayside reconnection layer and associated ion transport

H. Xie and Y. Lin

Physics Department, Auburn University, Auburn, Alabama

Abstract. The structure of the reconnection layer at the dayside magnetopause is studied by using a two-dimensional (2-D) hybrid code. The simulation domain is a rectangle in the xz plane around an X line at the magnetopause. In our previous study the guide magnetic field B_y was assumed to be zero. In the present simulation the effects of a finite B_y on the reconnection layer are studied. In addition, the influence of shear flows on the magnetic reconnection is also investigated. In the cases with a shear flow speed $\Delta V = 0$, as near the subsolar region, a large-amplitude rotational discontinuity is present on the magnetosheath side of the reconnection layer, across which the magnetic field changes direction from the magnetosheath to the magnetosphere. A high-speed accelerated flow is present on the magnetospheric side of the rotational discontinuity. For a higher-latitude reconnection in the Northern Hemisphere, where a shear flow is present across the magnetopause, the structure of the reconnection layer northward of the X line is very different from that southward. Northward of the X line, the rotational discontinuity with a larger field rotational angle exists on the magnetospheric side if the shear flow speed $\Delta V > 0.33(V_{Am} - V_{As})$, where V_{Am} and V_{As} are the Alfvén speeds in the magnetosphere and the magnetosheath, respectively. Below the X line, a thin, strong rotational discontinuity is always present on the magnetosheath side. By tracing the orbits of individual ion particles, we have performed a detailed analysis of ion transmission and reflection at the magnetopause. The average transmission (reflection) rate of the magnetosheath ions is found to be $\sim 85\%$ (15%). The reflection of the magnetosheath ions occurs mainly in the inner boundary layer.

1. Introduction

Magnetic reconnection [*Dungey*, 1961] is a fundamental mechanism for the transport of solar wind mass, momentum, and energy into the magnetosphere. The coupling between magnetospheric flows and the flows seen in the polar and auroral ionosphere is also largely affected by magnetic reconnections at the magnetopause [*Lockwood and Smith*, 1994]. Satellite observations at the dayside magnetopause [*Paschmann et al.*, 1979; *Sonnerup et al.*, 1981; *Gosling et al.*, 1990a, 1990b] have provided strong evidence for the existence of quasi-steady magnetic reconnection in the low-latitude (near-subsolar) magnetopause under a southward interplanetary magnetic field (IMF). Observations of high-latitude reconnections near the cusp magnetopause under northward IMF conditions are also reported for reconnections poleward or equatorward of the cusp [*Gosling et al.*, 1991; *Onsager and Fuselier*, 1994; *Fuselier et al.*, 1997, 2000; *Chandler et al.*, 1999].

Early theoretical models of steady state reconnection mainly include *Petschek*'s [1964] model for symmetric current sheet, applicable to the magnetotail current sheet, and *Levy et al.*'s [1964] asymmetric model for the dayside magnetopause, where the magnetospheric plasma density is assumed to be zero. Further theoretical studies based on the ideal magnetohydrodynamics (MHD) indicate that in general cases rotational discontinuities, slow shocks, slow expansion waves, and a contact discontinuity may exist in the outflow region [*Heyn et al.*, 1988; *Lin and Lee*, 1994a]. A primary large-amplitude rotational discontinuity bounds the reconnection layer from the magnetosheath side. In resistive MHD simulations the rotational discontinuity is replaced by an intermediate shock in the cases with a zero guide field ($B_y = 0$; coplanar magnetic field) or a time-dependent intermediate shock for $B_y \neq 0$ [*Lin and Lee*, 1994a].

Two-dimensional (2-D) resistive MHD simulations were also carried out to study the structure of the reconnection layer in the magnetosphere [*Sato*, 1979; *Ugai*, 1984; *Scholer*, 1989; *Shi and Lee*, 1990; *Lin and Lee*, 1999]. Slow shocks, intermediate shocks, and time-dependent intermediate shocks were found, although the MHD Rankine-Hugonuit (RH) jump conditions are not highly satisfied at slow shocks and intermediate shocks owing to the finite simulation domain [*Lin and Lee*, 1999].

MHD models and simulations, however, do not con-

Paper number 2000JA000143.
0148-0227/00/2000JA000143$09.00

sider the particle kinetic effects. In the efforts to include the kinetic effects, both one-dimensional (1-D) hybrid simulations and 2-D hybrid simulations, in which ions are treated as discrete particles and electrons are treated as a massless fluid, of magnetospheric reconnection layers have been performed in recent years. *Lin and Lee* [1994a] in their 1-D hybrid simulation indicate that the contact continuity disappears because of the mixing of ions along field lines. The slow shock and slow expansion wave are modified. The time-dependent intermediate shocks quickly evolve to a steady rotational discontinuity, and the intermediate shock exists only in the cases with $B_y = 0$. The existence of rotational discontinuities and associated high-speed flows is consistent with the satellite observations of quasi-steady reconnections at the magnetopause.

In 2-D reconnection in collisionless plasmas the reconnection requires the presence of a certain electric field in the diffusion region. This reconnection electric field may be generated because of electron inertia, nongyrotropic pressure, or other terms associated with the generalized Ohm's law [e.g., *Lyons and Pridemore-Brown*, 1990; *Cai et al.*, 1994; *Hesse et al.*, 1995; *Shay and Drake*, 1998]. Full-particle models which include both ion and electron dynamics [e.g., *Pritchett*, 1994; *Shay and Drake*, 1998] emphasize the physics of the X line, but they have numerical limitations for large-scale (ion scale) structures of the outflow region. Hybrid simulation models, on the other hand, can simulate the large-scale structure, although the physics of the X line associated with the electron particle dynamics cannot be included. *Hesse et al.* [1995] and *Kuznetsova and Hesse* [1995] developed a hybrid model for the self-consistent evolution of the full electron pressure tensor. In the present study and our previous simulations [*Lin and Xie*, 1997] the reconnection electric field is supplied explicitly by a resistive term in the diffusion region. Our main interest is in the large-scale structure of the reconnection layer, which is found to be not sensitive to the resistivity at the X line. Similar hybrid models have also been used for the reconnection layer in the distant magnetotail [e.g., *Lin and Swift*, 1996; *Lottermoser et al.*, 1998].

Lin and Xie [1997] carried out a 2-D hybrid simulation to study the formation and the structure of the dayside reconnection layer with $B_y = 0$. It was found that a quasi-steady structure develops behind a leading transient bulge in the reconnection. An intermediate shock bounds the reconnection layer from the magnetosheath side. The results are consistent with the 1-D hybrid simulations [*Lin and Lee*, 1994a]. *Krauss-Varban et al.* [1999] performed a similar 2-D hybrid simulation to study the formation of the magnetopause transition during reconnection and found some rotational discontinuity-like structure in the magnetopause. *Karimabadi et al.* [1999] used 2-D and three-dimensional hybrid simulations to investigate the formation of the core field (Hall field) within time-dependent plasmoids at the magnetopause and in the magnetotail. The magnetopause discontinuities in the cases with $B_y \neq 0$, however, have not been identified by the RH jump condition for quasi-steady reconnections.

An important condition that may affect the processes of magnetic reconnection is the presence of a finite magnetosheath flow, or the shear flow, at the magnetopause. Observations at the flank of the magnetopause by *Gosling et al.* [1986] have found that the structure of the boundary layer is quite different from the structure of the subsolar magnetopause, where the shear flow is nearly zero. A 1-D hybrid simulation [*Lin and Lee*, 1994b] and a 2-D MHD simulation [*La Belle-Hamer et al.*, 1995] have been performed to investigate the magnetic reconnection in the presence of a shear flow at the flank magnetopause. *La Belle-Hamer et al.* [1995] found that the reconnection ceases to develop for a sufficiently large magnetosheath flow speed $V_s > (V_{As} + V_{Am})$, where V_{As} and V_{Am} are the Alfvén speeds in the magnetosheath and the magnetosphere, respectively. In addition, *Lin and Lee* [1994b] found that there exists a threshold shear flow speed V^* such that in cases with $V_s < V^*$ ($V_s > V^*$) the rotational discontinuity with a larger field rotation exists on the magnetosheath (magnetospheric) side of the reconnection layer. The threshold speed is found to be $V^* = (V_{As} - V_{Am})$. The shear flow effects on the 2-D reconnection, however, have not been studied by using kinetic models.

The purpose of this paper is to systematically study the structure of the quasi-steady reconnection layer at the dayside magnetopause with the presence of a shear flow or a finite guide magnetic field ($B_y \neq 0$) by using a 2-D hybrid simulation code. The ion transmission and reflection at the magnetopause reconnection layer is also investigated by tracing orbits of individual particles. Our previous 2-D simulation [*Lin and Xie*, 1997] studied only the case with $B_y = 0$ and without the magnetosheath flow. It is shown in this paper that the presence of a finite magnetosheath flow and a finite guide field alters the structure of the magnetopause discontinuities significantly. The structure of reconnection layers above and below the X line is very different owing to the presence of the shear flow.

The organization of the paper is as follows. The simulation model is given in section 2. In section 3 the simulation results with $B_y \neq 0$ are presented. The results in the cases with $V_s \neq 0$ are shown in section 4. The ion transport across the magnetopause is discussed in section 5. A summary is given in section 6.

2. Simulation Model

A 2-D hybrid code [*Lin and Swift*, 1996; *Lin and Xie*, 1997] is used to study the structure of the reconnection layer at the dayside magnetopause. In the hybrid code,

ions are treated as discrete particles, and electrons are treated as a massless fluid. The simulation domain is a rectangle in the xz plane. Initially, the magnetopause current sheet is located at $x = 0$. The magnetosheath is in the region with $x > 0$, and the magnetosphere is in $x < 0$, where x is the normal direction of the current sheet. The antiparallel magnetic field is along the z direction, with $+z$ pointing to the north, and a common guide magnetic field is in the y (dawn-dusk) direction. The magnetic field component B_z, the ion number density N, and the temperature T have a smooth transition through the initial current sheet. Let the subscripts s and m denote quantities in the magnetosheath and magnetosphere, respectively. The initial z component magnetic field and plasma temperature are given by

$$B_{z0}(x) = \frac{1}{2}(B_{zm} + B_{zs}) + \frac{1}{2}(B_{zm} - B_{zs})\tanh(\frac{x}{\delta}), \quad (1)$$

$$T_0(x) = \frac{1}{2}(T_m + T_s) + \frac{1}{2}(T_m - T_s)\tanh(\frac{x}{\delta}), \quad (2)$$

where $\delta = \lambda_m$ is the half width of the initial current sheet, $\lambda_m = c/\omega_{pim}$ is the magnetospheric ion inertial length, c is the speed of light, and ω_{pim} is the ion plasma frequency in the magnetosphere. The ion number density is determined by the total pressure balance condition. The initial y component magnetic field is assumed to be constant. The z component plasma flow velocity is given by

$$V_{z0}(x) = \frac{1}{2}(V_{zm} + V_{zs}) + \frac{1}{2}(V_{zm} - V_{zs})\tanh(\frac{x}{\delta}), \quad (3)$$

where V_{zm} and V_{zs} are the magnetosheath and magnetospheric flow velocities, respectively, in the z direction. The simulation is carried out in the frame in which the magnetosheath flow velocity is assumed to be northward with $V_{zs} > 0$, the magnetospheric flow velocity is southward with $V_{zm} < 0$, and $|V_{zs}| = |V_{zm}|$. This reference frame is roughly the frame of the X line for the cases shown in this paper. This situation is applicable to the Northern Hemisphere. Our study does not emphasize the condition for the movement of the X line, but rather the structure of the discontinuity in the reconnection layer. The simulation results will be plotted in the Earth frame, in which the magnetospheric flow speed is zero.

In this paper we study the evolution of a spontaneous reconnection [*Scholer*, 1989]. A constant resistivity is imposed at the center of the domain, $(x, z) = (0, 0)$, to trigger the reconnection. The resistivity is modeled through a collisional term in the ion equation of motion and the electron's momentum equation. The collision frequency is assumed to be

$$\nu = \nu_0 \exp[-(x^2 + z^2)/\delta^2], \quad (4)$$

where $\nu_0 \sim$ 1-5Ω_m and Ω_m is the magnetospheric ion gyrofrequency. The initial ion temperature is assumed to be isotropic. The electron temperature, which is usually much lower than the ion temperature at the magnetopause, is assumed to be zero for simplicity.

At the outflow boundaries at $z = \pm L_z/2$ the plasma flow velocity is free. The magnetic field is extrapolated on the basis of a zero curl and a zero divergence of the field. At the inflow boundaries $x = \pm L_x/2$, B_x is set to be zero to assure a small separatrix angle of quasi-steady reconnection [*Yan et al.*, 1992], but the magnetic flux can convect into the simulation domain with the inflows induced by fast mode waves from the reconnection. Initially, there is no inflow velocity. The reason for not using a completely free magnetic field at the inflow boundary is that the inflow condition is partly determined by the magnetosheath field, which is carried by the magnetosheath plasma flow under a normal pressure.

In this paper the time t is normalized to Ω_m^{-1}. The magnetic field is in units of the magnetospheric field B_m, N is in units of the magnetospheric ion number density N_m, and T is in units of T_m. The velocity is normalized to the magnetospheric Alfvén speed V_{Am}, and the spatial coordinates are normalized to λ_m. The electric current density J is normalized to $B_m/(\mu_0\lambda_m)$.

3. Effects of a Finite B_y

In this section we present simulations for cases with a finite guide magnetic field $B_y \neq 0$. The shear flow speed is set to be zero. Three cases are shown in the following. A case with $B_y = 0$ is also shown briefly for comparison. In the simulation the number of ions per cell is chosen to be $N_s = 200$ on the magnetosheath side, and the density $N_m = 20$. The cell size $\Delta x = 0.3\lambda_m$, and $\Delta z = 0.6\lambda_m$. The size of the simulation domain is $L_x \times L_z = 60\lambda_m \times 200\lambda_m$, which corresponds to a system length of ± 1.1 R_E in the x direction and ± 3.5 R_E in the z direction for a magnetospheric density $N_m \sim 2$ cm^{-3}.

In case 1 the guide magnetic field $B_{ys} = B_{ym} = 0.3B_m$. The ratios of magnetic fields, plasma densities, and temperatures on the two sides of the initial current sheet are assumed to be $N_s/N_m = 10$, $B_s/B_m = 0.75$, and $T_s/T_m = 0.32$. The ion beta in the magnetosphere is set to be $\beta_m = 0.2$, and that in the magnetosheath is $\beta_s = 1.13$. Figure 1 shows the configuration of magnetic field lines, the ion velocity vectors, and contours of the density N at $t = 600\Omega_m^{-1}$. A quasi-steady reconnection layer has formed in the outflow region of the reconnection, while a leading bulge has moved out of the domain. The transient structure of the outflow region in collisionless reconnection at the magnetopause and in the magnetotail has been simulated by other hybrid simulations [*Hesse et al.*, 1995; *Lin and Xie*, 1997; *Lottermoser et al.*, 1998]. In the quasi-steady state of case 1, two rotational discontinuities have formed on the two sides of the reconnection layer. A strong rotational discontinuity, as indicated in Figure 1 by the dashed

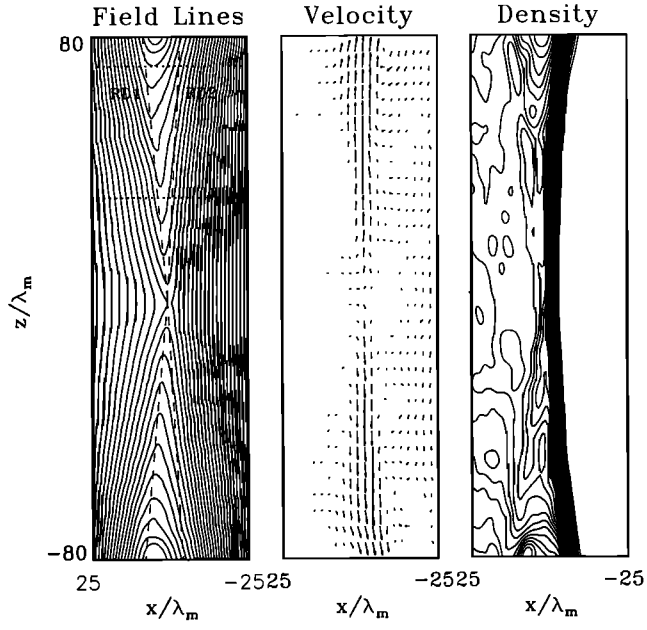

Figure 1. (left)Magnetic field lines, (middle)ion velocity vectors, and (right)a contour plot of ion number density N at $t = 600\Omega_m^{-1}$ in case 1 with $B_y = 0.3B_m$. The two dotted lines correspond to $z = z_1 = 30\lambda_m$ and $z = z_2 = 70\lambda_m$, respectively. Rotational discontinuities "RD1" and "RD2" are indicated by two dashed lines.

line labeled "RD1", is present on the magnetosheath side. A weak rotational discontinuity, labeled "RD2" in Figure 1, is present on the magnetospheric side. Across RD1 the B_z component of the magnetic field changes direction from the magnetosheath to the magnetosphere. The angle between the RD1 front and the z axis is 2.4°. Across RD2 the B_z component remains the direction of the magnetospheric field. The angle between the RD2 front and the z axis is 4.9°. The ion flows are greatly accelerated across RD1 and RD2 in the outflow region of the reconnection, as shown in the velocity vector plot.

Figure 2 shows hodograms of the tangential magnetic field (B_y and B_z) as x varies from the magnetosheath (negative B_z) to the magnetosphere (positive B_z) and spatial profiles of the normalized quantities B_y, B_z, ion flow velocity components V_y and V_z, parallel temperature $T_\parallel$ and perpendicular $T_\perp$, and density N at $t = 600\Omega_m^{-1}$ along x at $z = z_1 = 30\lambda_m$ and $z = z_2 = 70\lambda_m$. The two positions z_1 and z_2 are indicated by the two dotted lines in Figure 1. Note that x is normalized to λ_m, which is ~ 3.2 times of the magnetosheath ion inertial length λ_s. In Figure 2 the two rotational discontinuities RD1 and RD2 are indicated by the two vertical dotted lines through their center. The identification of RD1 and RD2 as rotational discontinuities is given below. Across RD1 at $z = z_2$ the tangential magnetic field rotates by $\sim 136°$ from negative to positive B_z, as shown in the field hodogram. The magnetic field strength B (not shown) and the density N are nearly constant. The flow components V_y and V_z increase corresponding to B_y and B_z, respectively. The parallel temperature increases in the reconnection layer owing to the mixing of the ions from the magnetosheath and the magnetosphere [*Lin and Xie*, 1997]. The perpendicular temperature also slightly increases across RD1. The RH jump conditions of rotational discontinuity are examined for the plasma with the anisotropic temperature [*Lin and Lee*, 1994a] and are found to be nearly satisfied at RD1, except that the velocity jump is smaller than the jump in the Alfvén velocity as predicted. The changes in V_y and V_z are nearly equal to 65% of the changes in Alfvén velocities V_{Ay} and V_{Az}, respectively. The smaller change in the flow velocity has also been found in the 2-D hybrid simulation of *Lin and Xie* [1997] and satellite observations at magnetopause rotational discontinuities [*Sonnerup et al.*, 1990]. Across RD2 the tangential magnetic field rotates by a small angle of 28°. The RH jump conditions of rotational discontinuity are nearly satisfied at RD2.

At the distance $z = z_1$, which is closer to the X line, RD1 and RD2 are closer in the x direction, as seen in Figure 2. The hodogram of the tangential magnetic field shows an S-shaped rotation of the magnetic field through RD1, with an electron sense (right-hand) rotation in the upstream, i.e., the magnetosheath side, and an ion sense (left-hand) rotation in the downstream. In RD2 the tangential magnetic field undergoes an electron sense rotation. The electron sense rotation of the magnetic field has also been found through the rotational discontinuities in the region with $z < 0$ below the X line.

Similar to our previous simulation for the case with $B_y = 0$ [*Lin and Xie*, 1997], no slow shocks are identified. The density and magnetic field strength changes monotonically in between RD1 and RD2 through the reconnection layer.

For comparison, the magnetic field hodogram and the spatial profiles of B_y, B_z, and N in case 2 initially with $B_y = 0$ are shown in Figure 3 . Similar to case 1, a strong discontinuity, across which the direction of the tangential magnetic field changes from the magnetosheath to the magnetosphere, is present on the magnetosheath side. The magnetic field is coplanar across this discontinuity, and thus the field rotation angle is equal to 180°. A slight density increase is seen across this discontinuity. A close examination indicates that the RH jump conditions of an intermediate shock, instead of rotational discontinuity, are nearly satisfied at this discontinuity [*Lin and Xie*, 1997], although the structures of the magnetic field and plasma quantities appear very similar to the rotational discontinuity RD1 in case 2 with $B_y \neq 0$. Therefore the finite B_y on the two sides of the initial current sheet results in the noncoplanar discontinuities, which are rotational discontinuities. The existence of quasi-steady discontinuities is consistent with satellite observations at the magne-

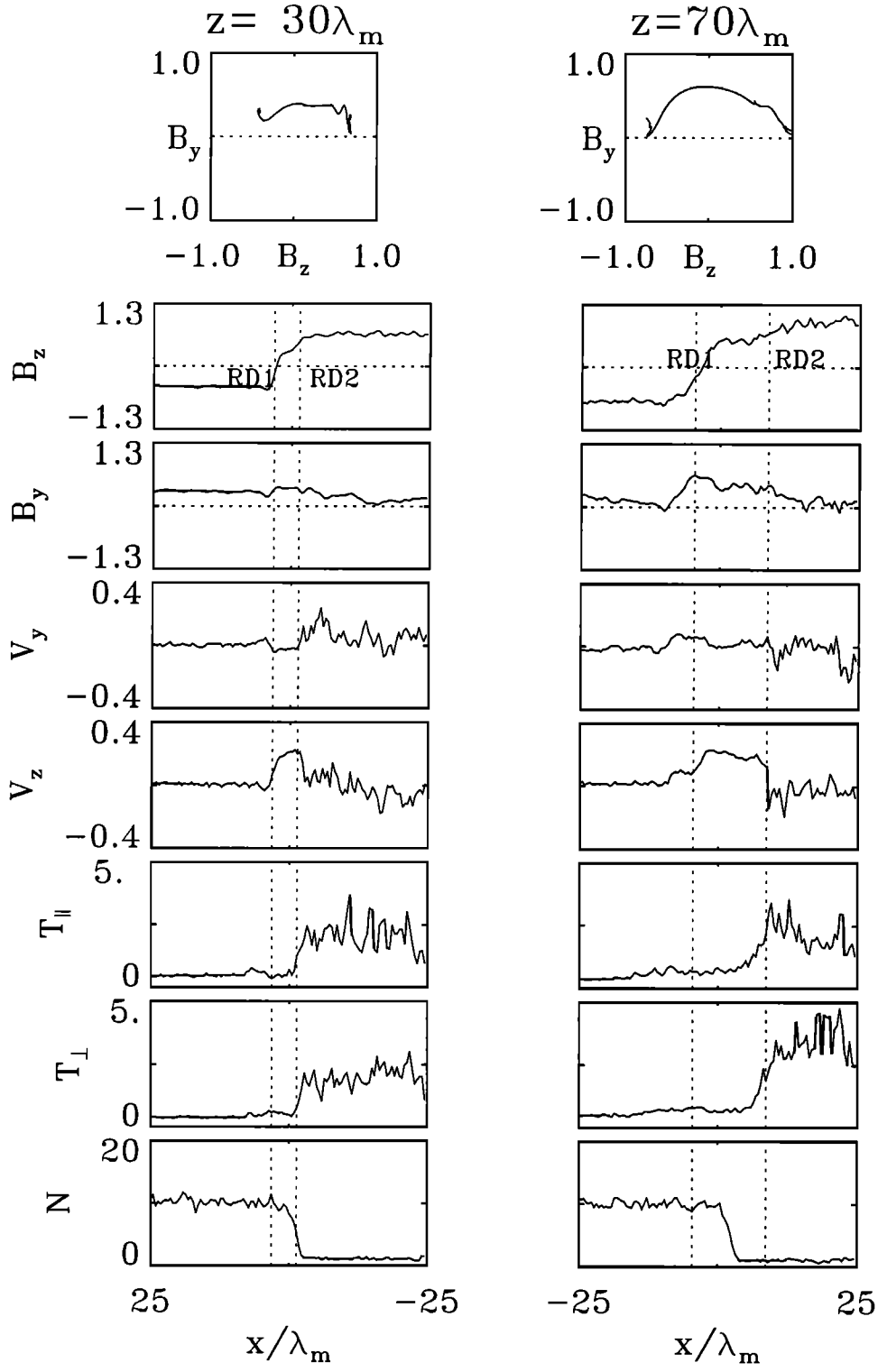

Figure 2. Hodograms of the tangential magnetic field and spatial profiles of B_y, B_z, V_y, V_z, $T_{\|}$, $T_{\perp}$, and N at $t = 600\Omega_m^{-1}$ as a function of x along $z = z_1$ and $z = z_2$ in case 1. The vertical dotted lines are through the discontinuities RD1 and RD2 in Figure 1.

topause [*Paschman et al.*, 1979; *Sonnerup et al.*, 1981; *Gosling et al.*,1990a,1990b].

Considering that the magnetic structure in the initial current sheet, i.e., a tangential discontinuity, may be complicated at the magnetopause [*Lee and Kan*, 1979; *Keyser and Roth*, 1998], we have also studied cases with various magnetic field profiles in the initial current sheet. In the following we show a case with a large initial magnetic field rotation. In case 3 the magnetic field and plasma quantities in the magne-

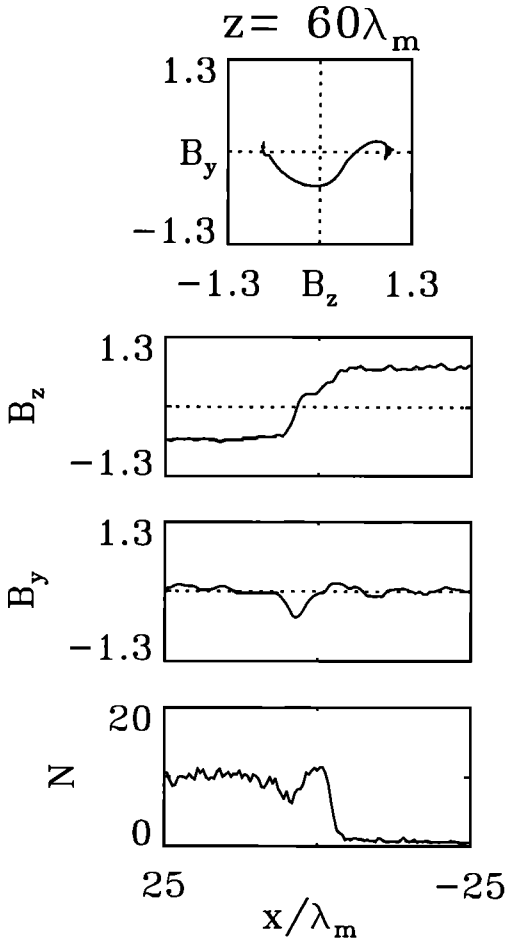

Figure 3. Hodogram of the tangential magnetic field and spatial profiles of B_y, B_z, and N at $t = 600\Omega_m^{-1}$ as a function of x at $z = 60\lambda_m$ in case 2 with $B_y = 0$.

tosheath and the magnetosphere are the same as in case 1, with $B_s = 0.75B_m$ and $B_{ys} = B_{ym} = 0.3B_m$, except that the magnetic field follows a large rotation angle of 240° > 180° (electron sense from magnetosheath to the magnetosphere). Similar to case 1, two rotational discontinuities RD1 and RD2 are formed in the reconnection layer. The top and bottom rows of Figure 4 show the magnetic field hodograms across the reconnection layer at $z = 30\lambda_m$ and $z = 50\lambda_m$, respectively. The left, middle, and right columns show the results at $t = 180\Omega_m^{-1}$, $300\Omega_m^{-1}$, and $450\Omega_m^{-1}$, respectively. At $t = 180\Omega_m^{-1}$ the rotational discontinuities have already formed at $z = 30\lambda_m$ but have not formed at farther distance $z = 50\lambda_m$. The tangential magnetic field is seen still following the large rotation angle through the reconnection layer at $z = 30\lambda_m$. At $t = 300\Omega_m^{-1}$ the field rotation angle through the reconnection layer at $z = 30\lambda_m$ has become < 180°, with $B_y > 0$ throughout the layer. Similar to case 1, an S-shaped field rotation is seen in RD1. The rotational discontinuities have also formed at $z = 50\lambda_m$, but the field rotation angle there is still > 180°. Finally, at $t = 450\Omega_m^{-1}$ the tangential magnetic field follows the short path in the hodogram at both the closer ($z = 30\lambda_m$) and the farther ($z = 50\lambda_m$) distance from the X line.

The structure of the rotational discontinuities obtained from our 2-D simulation is consistent with that from previous 1-D hybrid simulations [*Swift and Lee*, 1983; *Krauss-Varban*, 1993; *Lin and Lee*, 2000]: because of the ion orbits in the discontinuity, the rotational discontinuity tends to evolve to an equilibrium structure in which the magnetic field follows the smallest rotation angle (< 180°). In case 3 this evolution would

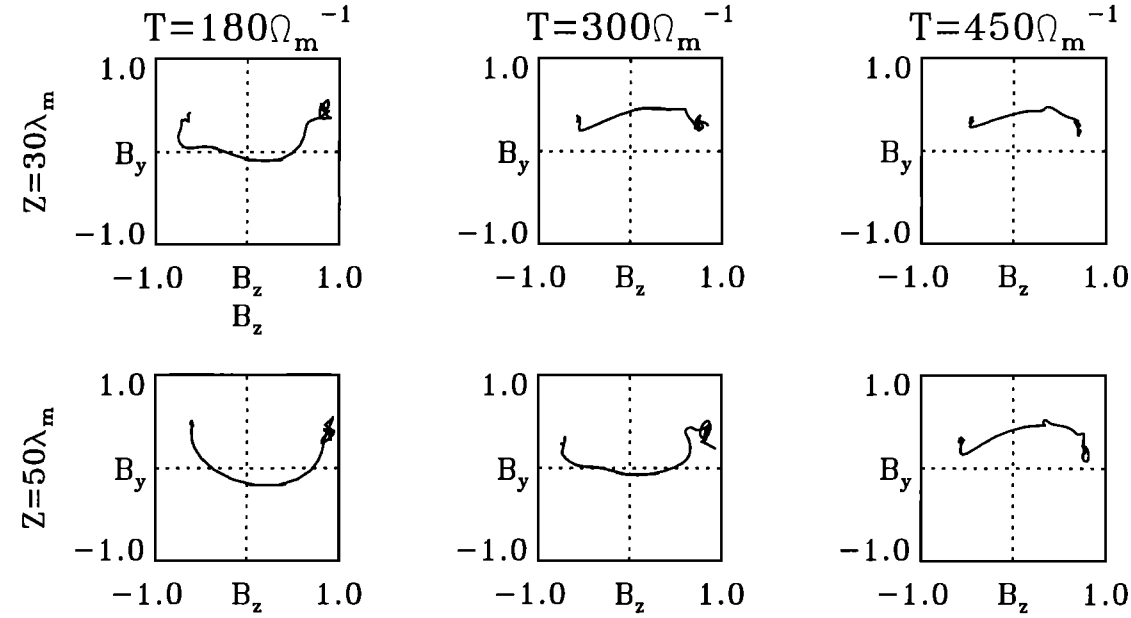

Figure 4. Magnetic field hodograms across the reconnection layer at $z = 30\lambda_m$ and $z = 50\lambda_m$ in case 3, in which the initial magnetic field follows a large rotation angle of 240°.

result in an ion sense field rotation from upstream to downstream. At the upstream edge, however, the magnetic field maintains an electron sense rotation, while the RD1 transition is dominated by the ion sense rotation, resulting in the S-shaped structure in RD1. The electron sense rotation at the magnetopause rotational discontinuity has been predicted by *Su and Sonnerup* [1968] using the first-order orbit theory and observed by *Sonnerup and Cahill* [1968]. The observation by *Berchem and Russell* [1982] from ISEE 1 and 2 magnetopause crossings showed that the magnetopause rotational discontinuity possesses a field rotation angle $< 180°$. The timescale for a rotation discontinuity with a field rotation angle $> 180°$ to evolve to a structure with a minimum rotation angle has been investigated by *Lin and Lee* [2000]. In case 3 the time for RD1 to reverse its field rotation sense is found to be $\sim 120\Omega_m^{-1}$. The width of the final equilibrium RD1 is $\sim 3\lambda_m$.

4. Effects of Shear Flows

In this section we present four cases with various shear flow speeds across the initial current sheet. The guide magnetic field B_y is assumed to be zero in the magnetosheath and the magnetosphere. The ratios of magnetic field, plasma densities , and temperature on the two sides are the same as in the previous cases. Since in general cases the discontinuities that bound the reconnection layer are rotational discontinuities, in the following we refer to the discontinuities on the magnetosheath and the magnetospheric sides as RD1 and RD2, respectively, even though they may be an intermediate shock in the cases with $B_y = 0$.

Figure 5b shows the configuration of field lines, ion velocity vectors, and contours of the field-aligned currents in case 4 with shear flow speed $\Delta V \equiv V_{zs} - V_{zm} = 0.2V_{As} = 0.05V_{Am}$ at $t = 600\Omega_m^{-1}$. The results in case 2 with $\Delta V = 0$ are shown in Figure 5a for comparison. Note that the velocities are plotted in the Earth frame. In case 2 the structure of the reconnection layer is nearly symmetric above ($z > 0$) and below ($z < 0$) the X line, while in case 4 with a shear flow across the magnetopause the structure of the reconnection layer above the X line is very different from that below the X line. The accelerated flow in the steady state reconnection layer has a speed above the X line higher than that below the X line in the X line frame. This difference in the convection speed is due to the fact that the magnetosheath flow velocity is parallel to the direction of the magnetic tension force across the primary rotational RD1 above X line but is antiparallel to the tension force below the X line. Therefore in case 4 the magnetosheath flow is accelerated above the X line, as seen from the northward (positive z) flow vectors in the $z > 0$ region in the reconnection layer, while the flow is decelerated and turned southward below the X line. In case 4 the convection speeds at the center of the reconnection layer are found to be nearly $0.38V_{Am}$ above the X line and $0.12V_{Am}$ below the X line in the Earth frame. The formation of the reconnection layer above the X line is also faster than that below the X line, as seen from Figure 5b, in which the leading bulge has not

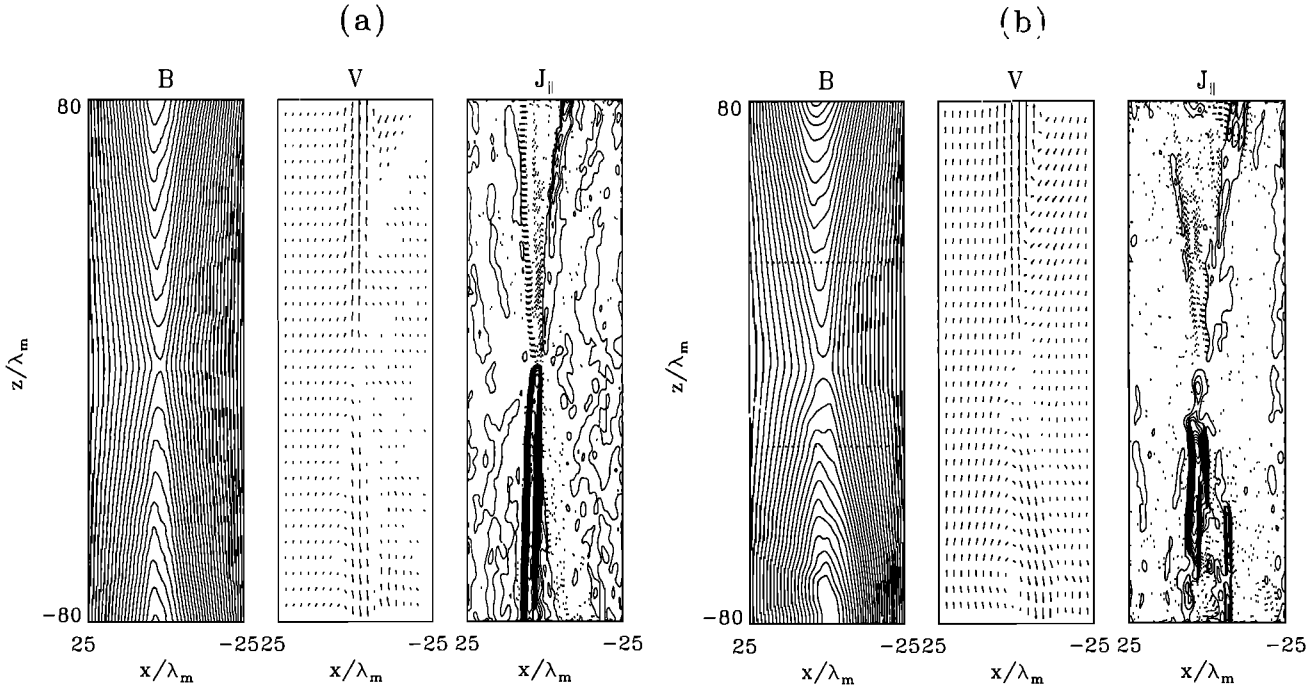

Figure 5. (a)(left)Magnetic field lines, (middle)ion velocity vectors, and (right)contours of the field-aligned current density $J_\parallel$ at $t = 600\Omega_m^{-1}$ in case 2 with $\Delta V = 0$. (b)results at $t = 600\Omega_m^{-1}$ in case 4 with $\Delta V = 0.2V_{As}$. The dotted lines correspond to $z = 30\lambda_m$ and $z = -26\lambda_m$.

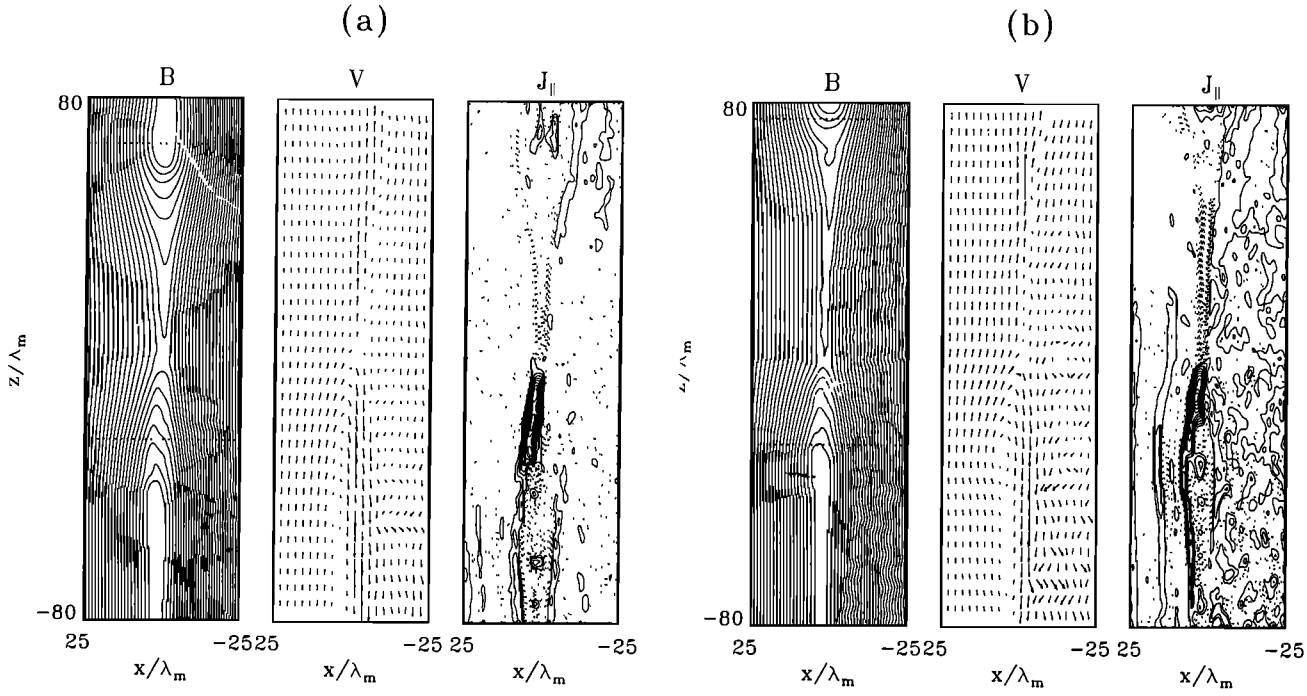

Figure 6. (a) (left)Magnetic field lines, (middle)ion velocity vectors, and (right)contours of $J_\parallel$ at $t = 600\Omega_m^{-1}$ in case 5 with $\Delta V = 1.0V_{As}$. The dotted lines correspond to $z = z_1 = 40\lambda_m$ and $z = -25\lambda_m$. (b)results at $t = 600\Omega_m^{-1}$ in case 6 with $\Delta V = 1.4V_{As}$. The dotted lines correspond to $z = z_1 = 64\lambda_m$ and $z = -25\lambda_m$.

convected out of the simulation domain in the $z < 0$ region, while the steady reconnection layer has formed in the entire $z > 0$ region.

In both case 2 and case 4 a strong field-aligned current density $J_\parallel$ is seen in RD1 on the magnetosheath side, as seen in Figure 5. The solid (dotted) contour lines indicate positive (negative) $J_\parallel$. The existence of the parallel currents is due to the finite B_y oscillations in the rotational discontinuity, which is caused by the Hall effects associated with the finite ion Larmor radii. The perpendicular currents in RD1 are also stronger than that in RD2. In the cases with $B_y = 0$ in the magnetosheath and the magnetosphere, the rotation in the magnetic field is right-handed in the magnetopause rotational discontinuities. Therefore $J_\parallel < 0$ ($J_\parallel > 0$) above or northward (below or southward) of the X line. These currents correspond to upward field-aligned currents in the ionosphere in both Northern and Southern Hemispheres. On the other hand, in RD2, $J_\parallel > 0$ ($J_\parallel < 0$) above (below) the X line. Note that in the cases with $B_y > 0$, $J_\parallel$ in the final structure of both RD1 and RD2 above or below the X line is positive. The sense of $J_\parallel$ is reversed for $B_y < 0$ on the two sides of the magnetopause current layer. The generation of Alfvén mode waves and the associated $J_\parallel$ in dayside reconnection has also been shown by 3-D MHD simulations [e.g., *Ma and Lee*, 1999]. The dominant senses of $J_\parallel$ for $B_y > 0$ and $B_y < 0$ are similar to those obtained in our hybrid simulation, but the Hall effect and the evolution of magnetic field due to the ion dynamics cannot be studied by the MHD model.

The strength of the primary rotational discontinuity RD1 (secondary RD2) is reduced (enhanced) by the presence of the sheath flow. Figure 6a shows magnetic field lines, flow velocities, and contours of the parallel currents at $t = 450\Omega_m^{-1}$ in case 5 with $\Delta V = 1.0V_{As} = 0.25V_{Am}$. Above the X line the positions where the field lines kink at various z distances exist nearly at the central x locations in the reconnection layer, whereas in case 2 with $\Delta V = 0$ the magnetopause current layer is largely concentrated in RD1 on the magnetosheath side. In case 4, although the magnetopause current layer exists in the entire width (along x) of reconnection layer in $z > 0$, the total width of this reconnection layer appears narrower than that in case 2 because the convection speed of the field lines along the magnetopause is faster. Figure 6b depicts the results in case 6 with $\Delta V = 1.4V_{As} = 0.35V_{Am}$. The location associated with a sharp change in the magnetic field direction at various distance z has shifted to the magnetospheric side of the reconnection layer. Below the X line, however, a large-amplitude RD1 still exists on the magnetosheath side in both case 5 and case 6.

The left, middle, and right columns of Figure 7a show the spatial profiles of quantities B_z, V_z, $T_\parallel$ (solid lines), and $T_\perp$ (dotted lines) in case 4, case 5, and case 6, respectively, in the reconnection layer above the X line. The results are shown for $t = 600\Omega_m^{-1}$ along the dotted lines in the $z > 0$ regions in Figures 5 and 6. In case 4 with $\Delta V = 0.2V_{As}$, the B_z component changes sign across RD1, similar to case 2 without shear flows. In case 5 with $\Delta V = 1.0V_{As}$, B_z is reduced to ~ 0

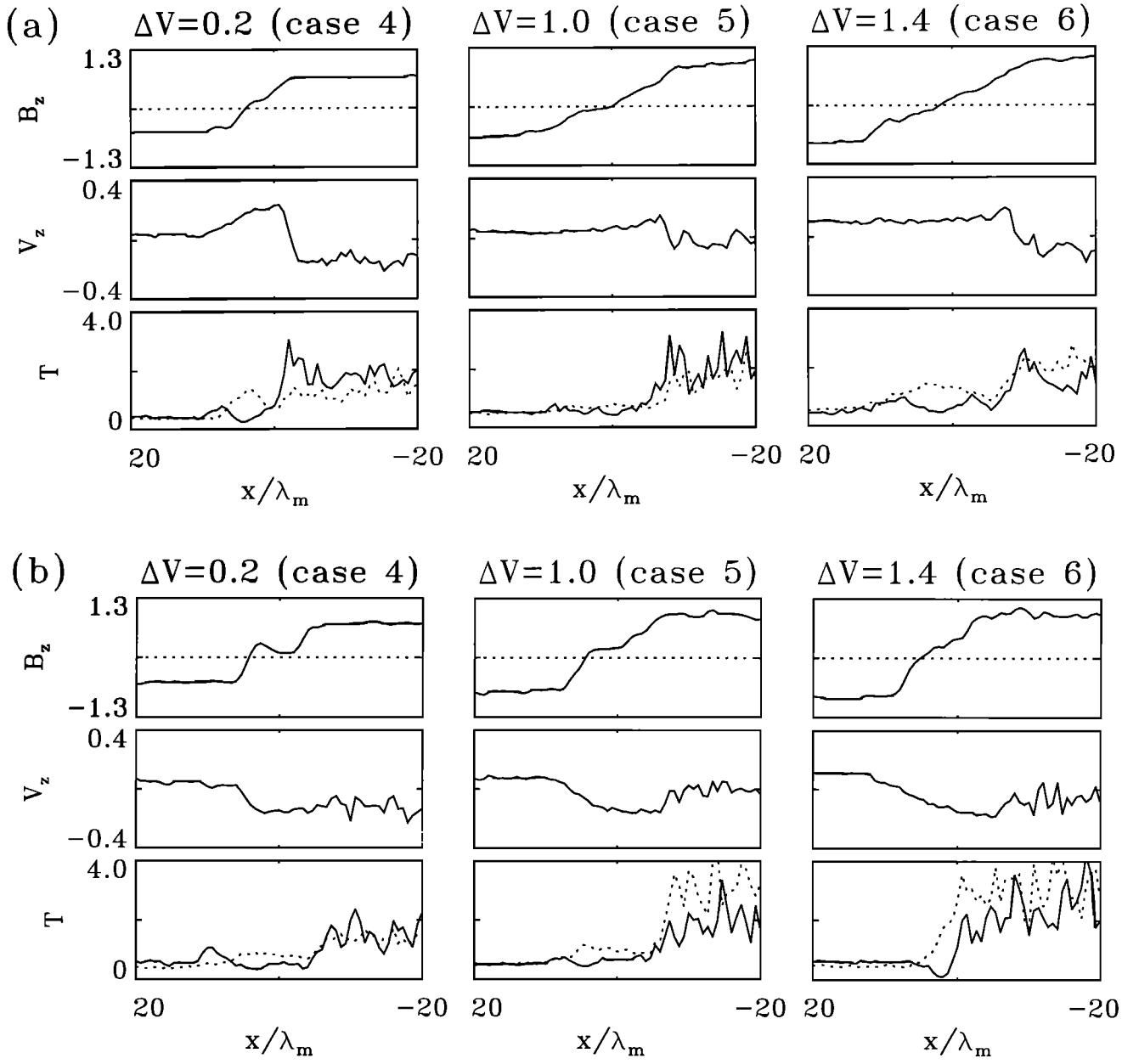

Figure 7. (a)Spatial profiles of B_z, V_z, $T_{||}$ (solid lines), and $T_{\perp}$ (dotted lines) in cases 4, 5, and 6 along the corresponding dotted lines above the X line in Figures 5 and 6. (b) Results in (left)case 4, (middle)case 5, and (right)case 6 along the corresponding dotted lines in Figures 5 and 6 below the X line.

at the center of the reconnection layer from both the magnetosheath and the magnetosphere. As the shear flow further increases to $\Delta V = 1.4V_{As}$ in case 6, the larger- (smaller-) amplitude rotational discontinuity has shifted to the location of RD2 (RD1). Note that in cases 5 and 6 the flow acceleration across RD1 is weak, while a sharp increase in V_z is seen on the magnetospheric side.

Note that in the cases with $B_y = 0$ on the two sides of the boundary layer, the negative (positive) $J_{||}$ remains to dominate the reconnection layer above (below) the X line, regardless of the magnitude of the shear flow speed. *Sonnerup* [1979] suggested a B_y perturbation that is consistent with such a sense of $J_{||}$ due to the finite inertia of the ions coming into the magnetopause near the X line. An opposite B_y perturbation was also predicted for the ions from the magnetosphere. Since the ion density in the magnetosphere is very low, the dominant sense of B_y in the current layer should be that due to the magnetosheath ions, as seen in the above cases. A similar sense of the polarization in B_y has also been shown by *Karimabadi et al.* [1999] for the structure of transient magnetopause reconnections. Our simulation further shows that the polarizations of B_y above and below the X line in the quasi-steady discontinuities are not affected by the existence of the shear flows. In the

cases with a noncoplanar B_y the magnetic field in rotational discontinuities always evolves toward a minimum field rotation angle, and thus the sense of B_y in the current layer is also not altered by shear flows.

The left, middle, and right columns of Figure 7b show the spatial profiles along the dotted lines in Figures 5 and 6 below the X line in Figures 5 and 6 for cases 4, 5, and 6, respectively. It is seen that the stronger rotational discontinuity exists on the magnetosheath side in all of these cases. The V_z component is negative at the center of the reconnection layer. It is seen from the above cases that a threshold shear flow speed V^* exists, such that for $\Delta V < V^*$ the stronger rotational discontinuity exists on the magnetosheath side and that for $\Delta V > V^*$ the stronger rotational discontinuity is present on the magnetospheric side. This result is consistent with the 1-D hybrid simulation of *Lin and Lee* [1994b]. The threshold speed in our 2-D simulation is found to be $V^* \simeq 1.0V_{As} \simeq 0.33(V_{Am} - V_{As})$, corresponding to case 5. Case 6 is thus associated with $\Delta V > V^*$. The existence of the threshold shear flow speed can be understood from the jump conditions of plasma flow velocities across the discontinuities [*Lin and Lee*, 1994b]. Owing to a high density and a low magnetic field in the magnetosheath, a large-amplitude RD1 is required to accelerate plasma from the inflow to the outflow region on the magnetosheath side. In the presence of the magnetosheath flow, however, the change of the tangential velocity from the inflow region to the outflow region is decreased, and thus RD1 is weaker. At $\Delta V \simeq V^*$ the field amplitude of RD1 is nearly the same as that of RD2.

Note that the threshold speed obtained in the isotropic MHD model is $V^* = (V_{Am} - V_{As})$. Owing to the effects of the temperature anisotropy, the threshold speed found in the 1-D hybrid simulation by *Lin and Lee* [1994b] is $V^* \simeq 0.6(V_{Am} - V_{As})$, which is smaller than that in the MHD model. In our 2-D simulation the threshold speed is found to be even smaller, nearly equal to $0.33(V_{Am} - V_{As})$. This smaller speed is due to the fact that the velocity change across the rotational discontinuities in the 2-D hybrid simulation is smaller than that predicted from the Walen relation, as discussed for case 1.

It is found that the X line moves northward away from the central diffusion region in the simulation frame if $\Delta V > 1.8V_{As}$. For $\Delta V = 2.0V_{As}$, or the magnetosheath flow speed $V_{zs} = V_{As}$, the X line moves with a speed of $\sim 0.18V_{Am}$ in the simulation frame. *La Belle-Hamer et al.* [1995] has argued using an MHD simulation that a noticeable motion of the X line occurs if the magnetosheath flow speed relative to the X line is greater than V_{As}. A similar result is obtained in our hybrid simulation. The motion of the X line can be understood as follows. As the shear flow speed increases, the separatrix angle of the reconnection is getting large below the X line, while it is smaller above the X line, as seen in Figures 5 and 6. If the outflow speed V_{out} below the X line, which is determined by the magnetic tension force and the resistivity, is so small relative to the X line that the separatrix angle below the X line approaches 90°, the net Poynting flux into the diffusion region becomes zero. Thus the stable X line cannot be maintained. On the other hand, the fast removal of the plasma above the X line results in a thinner current layer in the $z > 0$ region. The X line then easily moves to a new location in the positive z direction.

5. Ion Transmission and Reflection at the Magnetopause Reconnection Layer

Our simulation shows that the majority of the incident magnetosheath ions are transmitted through the magnetopause rotational discontinuity RD1 into the boundary layer, while a relatively small part of the magnetosheath ions are reflected back into the magnetosheath. We have traced the particle trajectories to identify the transmission rate and the reflection rate of the magnetosheath ions.

Because of the existence of two rotational discontinuities in general cases, the ions can be reflected at either RD1 or RD2. The particle trajectories are found to be complicated. In our calculation the trajectories are followed for particles at various distances z both above and below the X line from $t = 0$ to $t = 600\Omega_m^{-1}$. Figure 8 shows some typical ion orbits of a group of the magnetosheath ions in case 4, in which $\Delta V = 0.2V_{As}$. Initially, these ions are located near $(x, z) = (7\lambda_m, -16\lambda_m)$, as marked by the cross sign in Figure 8. They are seen to be incident onto the magnetopause reconnection layer. Also shown in Figure 8 are the magnetic field lines at $t = 600\Omega_m^{-1}$. Five different types of the orbits are shown. Orbit 1 and orbit 2 represent the particles that have transmitted into the magnetosphere from the magnetosheath side across the current layer, as shown by the dotted lines in Figure 8. Particle 1 has penetrated into the magnetosphere from a location below the X line, while particle 2 has penetrated from a location above the X line. On the other hand, the particles following orbit 3 and orbit 4 have been reflected back into the magnetosheath from the discontinuities, as shown by the solid trajectory curves in Figure 8. Again, the particles can be reflected either above or below the X line if they are initially not too far away from the X line. Orbit 5 represents a particle that has penetrated through RD1 but is trapped in the outflow region at the final moment, as shown by the dashed-dotted curve. Note that the field lines are constantly carried away from the X line by the outflow while the ions are traced.

The average transmission rate either above or below the X line is estimated by identifying the final locations of the magnetosheath ions that are incident onto the magnetopause at various distances of z. The magnetosheath particles initially near $x = 10\lambda_m$ and $|z| = 10$, 30, and $60\lambda_m$ within a box of $\delta x = 5\lambda_m$ and $\delta z = 5$ are traced. Only those particles actually incident on

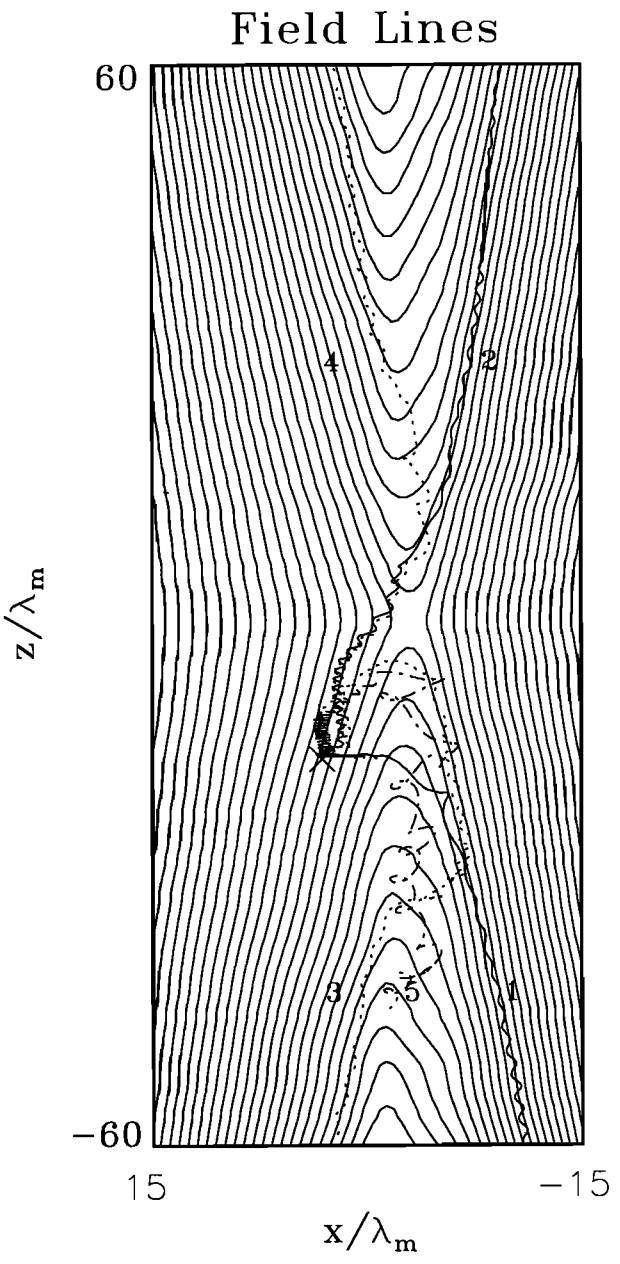

Figure 8. Some typical orbits of the magnetosheath ions in case 4 with $\Delta V = 0.2V_{As}$ from $t = 0$ to $t = 600\Omega_m^{-1}$.

the current layer are counted. We have also traced the magnetosheath particles from other x distances near the current layer at $t = 0$ and traced particles from various times. A similar transmission rate is obtained. A total of 40,000 particles have been traced for each case.

We take the transmitted particles as those that have passed RD1 from the magnetosheath by $t = 600\Omega_m^{-1}$, and the reflected ions are taken as those that end up with a location in the magnetosheath. In the case without a shear flow, i.e., $\Delta V = 0$, the transmission rate is estimated to be $\sim$ 85%, and reflection rate is $\sim$ 15%. In addition, a detailed examination indicates that the reflection rate at a distance z farther from the X line is higher than that near the X line. For example, at $z \simeq 65\lambda_m$ the reflection (transmission) rate is $\sim$ 20% (80%), whereas at $z \simeq 10\lambda_m$ the reflection (transmission) rate is $\sim$ 5% (95%). Some ions are reflected at the kinked magnetic field lines in the reconnection layer. Nevertheless, it is found that the reflection of the ions occurs mainly in the inner boundary layer. Most of the incident ions from the magnetosheath can penetrate through RD1 on the magnetosheath side of the current layer, which is consistent with the hybrid simulation of *Swift and Lee* [1983] for an isolated magnetopause rotational discontinuity. These ions then drift along the magnetopause. If the ions encounter an increase of the magnetic field, their drift velocity will decrease owing to the mirror force and be reflected back at the inner boundary layer into the magnetosheath field. In addition, some incident ions from the magnetosheath are found to be reflected at the X line. The reflection rate under various β_s will be studied elsewhere.

In the presence of a shear flow the transmission or reflection rate above the X line is found to be different from that below the X line. In case 4 with $\Delta V = 0.2V_{As}$, the reflection (transmission) rate is estimated to be $\sim$ 24% (76%) in the reconnection layer region below the X line. Above the X line the reflection rate is found to be $\sim$ 12%, while the transmission rate is $\sim$ 88%. The difference between the transmission rates above and below the X line is due to the difference in the magnetic configuration. Overall, the magnetic curvature radius in the $z > 0$ region is larger than that in $z < 0$ in the cases with a shear flow, as seen in Figures 5 and 6. It is known that the ion orbits in the magnetic field are controlled by the curvature parameter $\kappa = (R_{\min}/\rho_{\max})^{1/2}$, where $R_{\min}$ is the minimum radius of curvature of the magnetic field and $\rho_{\max}$ is the maximum Larmor radius of ions [*Buchner and Zelenyi*, 1989]. The reflected ions are found to have a relatively large Larmor radius or a relatively small value of κ. The ions with a Larmor radius much smaller than the radius of curvature of the magnetic field are strongly magnetized and simply transmitted through the current sheet along the field lines. Below the X line, sharp kinks of field lines are seen in RD1 on the magnetosheath side. Therefore the reflection rate is higher below the X line.

6. Summary

In summary, a 2-D hybrid simulation has been carried out to study the structure of the dayside magnetopause reconnection layer. In particular, the effects of a finite guide field B_y and a shear flow are investigated. The simulation is carried out in the frame in which the magnetosheath and the magnetospheric plasmas have an equal but opposite flow velocity along the north-south direction. The main results are summarized below.

1. In the presence of a finite guide magnetic field $B_y \neq 0$ in the magnetosheath and the magnetosphere,

two rotational discontinuities are present in the reconnection layer, whereas in our previous study for $B_y = 0$ an intermediate shock, instead of rotational discontinuities, is present. In cases without a shear flow a large-amplitude rotational discontinuity RD1 bounds the reconnection layer from the magnetosheath side, and a much weaker rotational discontinuity RD2 exists on the magnetospheric side. The plasma is accelerated by the rotational discontinuities, consistent with satellite observations [e.g., *Sonnerup et al.*, 1981].

2. The polarization of the tangential magnetic field appears to be right-handed (in electron sense) on the upstream side of the rotational discontinuity, in which the shock normal angle is large. In the cases with $B_y = 0$ on the two sides of the initial current sheet, a large-amplitude right-handed rotation is present in the magnetic field in RD1. In the cases with $B_y \neq 0$ the rotational discontinuity evolves to a final structure in which the magnetic field follows a shortest ($< 180°$) rotation angle. In the cases with a tangential field rotation angle $> 180°$ across the initial current sheet, the field rotation reverses, and the net rotation angle turns to be $< 180°$ in a time of $\Delta t \sim 120\Omega_m^{-1}$ after a local reconnection layer has formed. The structure of rotational discontinuities obtained in our 2-D simulation is consistent with previous hybrid simulations of rotational discontinuities [e.g., *Swift and Lee*, 1983; *Krauss-Varban*, 1993; *Lin and Lee*, 2000]. Associated with the perturbations in B_y, field-aligned currents $J_\parallel$ are generated in the reconnection layer.

3. In the presence of a shear flow across the magnetopause, the structure of the reconnection layer above the X line ($z > 0$; northward) is found to be very different from that below the X line ($z < 0$). The formation of the reconnection layer above the X line is faster than that below the X line because the shear flow (magnetosheath flow) enhances the convection speed on the northward side. Above the X line the rotational discontinuity with a larger field rotational angle exists on the magnetospheric side if the shear flow speed is larger than a threshold value $V^* \simeq 0.33(V_{Am} - V_{As})$. For a shear flow $\Delta V \geq V^*$ the magnetopause current layer appears thick above the X line. Below the X line the rotational discontinuity RD1 on the magnetosheath side is thin and always stronger than RD2. For a certain guide field B_y (zero or nonzero), however, the dominant senses of $J_\parallel$ above and below the X line remain similar for different shear flow speeds.

4. If the magnetosheath flow speed is greater than a value $\sim V_{As}$ in the simulation frame, the X line moves in the direction of the magnetosheath flow in this frame.

5. In the case without the shear flow, i.e., $\Delta V = 0$, the average transmission rate of the magnetosheath ions is found to be $\sim 85\%$, and the reflection rate is $\sim 15\%$. In addition, the reflection rate near the X line is smaller than that farther from the X line. In the cases with a shear flow speed $\Delta V \neq 0$ the reflection rate above the X line is, in general, smaller than that below the X line.

Acknowledgments. This work was supported by NASA grant NAG5-8081 and NSF grant ATM-9805550 to Auburn University. Computer resources were provided by the National Partnership for Advanced Computational Infrastructure and the Alabama Supercomputer Center.

Janet G. Luhmann thanks the referees for their assistance in evaluating this paper.

References

Berchem, J., and C. T. Russell, Magnetic field rotation through the magnetopause: ISEE 1 and 2 observations, *J. Geophys. Res., 87*, 8139, 1982.

Buchner, J., and L. M. Zelenyi, Regular and chaotic charged particle motion in magnetotaillike field reversals, 1, Basic theory of trapped motion, *J. Geophys. Res., 94*, 11,821, 1989.

Cai, H. J., D. Q. Ding, and L. C. Lee, Momentum transport near a magnetic X line in collisionless reconnection, *J. Geophys. Res., 99*, 35, 1994.

Chandler, M. O., S. A. Fuselier, M. Lockwood, and T. E. Moore, Evidence of component merging equatorward of the cusp, *J. Geophys. Res., 104*, 22,623, 1999.

Dungey, J. W., Interplanetary magnetic field and the auroral zones, *Phys. Rev. Lett., 6*, 47, 1961.

Fuselier, S. A., B. J. Anderson, and T. G. Onsager, Electron and ion signatures of field line topology at the low-shear magnetopause, *J. Geophys. Res., 102*, 4847, 1997.

Fuselier, S. A., S. M. Petrinec, and K. J. Trattner, Stability of the high-latitude reconnection site for steady northward IMF, *Geophys. Res. Lett., 27*, 473, 2000.

Gosling, J. T., M. F. Thomsen, S. J. Bame, and C. T. Russell, Accelerated plasma flows at the near-tail magnetopause, *J. Geophys. Res., 91*, 3029, 1986.

Gosling, J. T., M. F. Thomsen, S. J. Bame, R. C. Elphic, and C. T. Russell, Cold ion beams in the low latitude boundary layer during accelerated flow events, *Geophys. Res. Lett., 17*, 2245, 1990a.

Gosling, J. T., M. F. Thomsen, S. J. Bame, T. G. Onsager, and C. T. Russell, The electron edge of the low latitude boundary layer during accelerated flow events, *Geophys. Res. Lett., 17*, 1833, 1990b.

Gosling, J. T., M. F. Thomsen, S. J. Bame, R. C. Elphic, and C. T. Russel, Observations of reconnection of interplanetary and lobe magnetic field lines at the high-latitude magnetopause, *J. Geophys. Res., 96*, 14,097, 1991.

Hesse, M., D. Winske, and Masha M. Kuznetsova, Hybrid modeling of collisionless reconnection in two-dimensional current sheets: Simulations, *J. Geophys. Res., 100*, 21,815, 1995.

Heyn, M. F., H. K. Biernat, R. P. Rijnbeek, and V. S. Semenov, The structure of reconnection layer, *J. Plasma Phys., 40*, 235, 1988.

Karimabadi, H., D. Krauss-Varban, N. Omidi, and H. X. Vu, Magnetic structure of the reconnection layer and core field generation in plasmoids, *J. Geophys. Res.,104*, 12,313, 1999.

Keyser, J. D., and M. Roth, Magnetic field rotation at the dayside magnetopause: AMPTE/IRM observations, *J. Geophys. Res., 103*, 6663, 1998.

Krauss-Varban, D., Structure and length scales of rotational discontinuities, *J. Geophys. Res., 98*, 3907, 1993.

Krauss-Varban, D., H. Karimabadi, and N. Omidi, Two-dimensional structure of the co-planar and non-coplanar magnetopause transition during reconnection, *Geophys. Res. Lett., 26*, 1235, 1999.

Kuznetsova, M. M., and M. Hesse, Hybrid modeling of the tearing instability in collisionless two-dimensional current

sheets: Linear theory, *J. Geophys. Res., 100*, 21,827, 1995.

La Belle-Hamer, A. L., A. Otto, and L. C. Lee, Magnetic reconnection in the presence of sheared flow and density asymmetry: Applications to the Earth's magnetopause, *J. Geophys. Res., 100*, 11,875, 1995.

Lee, L. C., and J. R. Kan, A unified kinetic model of the tangential magnetopause structure, *J. Geophys. Res., 84*, 6417, 1979.

Levy, R. H., H. E. Petschek, and G. L. Siscoe, Aerodynamic aspects of magnetospheric flow, *AIAA J., 2*, 2065, 1964.

Lin, Y., and L. C. Lee, Structure of reconnection layers in the magnetosphere, *Space Sci. Rev., 65*, 59, 1994a.

Lin, Y., and L. C. Lee, Reconnection layer at the flank magnetopause in the presence of shear flow, *Geophys. Res. Lett., 21*, 855, 1994b.

Lin, Y., and L. C. Lee, Reconnection layers in two-dimensional magnetohydrodynamics and comparison with one-dimensional Riemann problem, *Phys. Plasmas, 6*, 3131, 1999.

Lin, Y., and L. C. Lee, Magnetic field rotation and transition width in rotational discontinuities and Alfvén wave trains, *J. Geophys. Res., 105*, 139, 2000.

Lin, Y., and D. W. Swift, A two-dimensional hybrid simulation of the magnetotail reconnection layer, *J. Geophys. Res., 101*, 19,859, 1996.

Lin, Y., and H. Xie, Formation of reconnection layer at the dayside magnetopause, *Geophys. Res. Lett., 24*, 3145, 1997.

Lockwood, M., and M. F. Smith, Low and middle altitude cusp particle signatures for general magnetopause reconnection rate variations, 1, Theory, *J. Geophys. Res., 99*, 8531, 1994.

Lottermoser, R. F., M. Scholer, and A. P. Matthews, Ion kinetic effects in magnetic reconnection: Hybrid simulations, *J. Geophys. Res., 103*, 4547, 1998.

Lyons, L. R., and D. C. Pridemore-Brown, Force balance near an X line in a collisionless plasma, *J. Geophys. Res., 95*, 20,903, 1990.

Ma, Z. W., and L. C. Lee, A simulation study of generation of field-aligned currents and Alfvén waves by three-dimensional magnetic reconnection, *J. Geophys. Res., 104*, 10,117, 1999.

Onsager, T. G., and S. A. Fuselier, The location of magnetic reconnection for northward and southward interplanetary magnetic field, in *Solar System Plasmas in Space and Time, Geophys. Monogr. Ser.*, vol. 84, edited by J. L. Burch and J. H. Waite Jr., pp. 183-197, AGU, Washington, D. C., 1994.

Paschmann, G., B. U. O. Sonnerup, I. Papamastorakis, N. Sckopke, G. Haerendel, S. J. Bame, J. R. Asbridge, J. T. Gosling, C. T. Russell, and R. C. Elphic, Plasma acceleration at the Earth's magnetopause: Evidence for reconnection, *Nature, 282*, 243, 1979.

Petschek, H. E., Magnetic field annihilation, in *AAS-NASA Symposium on the Physics of Solar Flares, NASA Spec. Publ., SP-50*, 425, 1964.

Pritchett, P. L., Effect of electron dynamics on collisionless reconnection in two-dimensional magnetotail equilibria, *J. Geophys. Res., 99*, 5935, 1994.

Sato, M., Strong plasma acceleration by slow shocks resulting from magnetic reconnection, *J. Geophys. Res., 84*, 7177, 1979.

Scholer, M., Undriven magnetic reconnection in an isolated current sheet, *J. Geophys. Res., 94*, 8805, 1989.

Shay, M. A., and J. F. Drake, The role of electron dissipation on the rate of collisionless magnetic reconnection, *Geophys. Res. Lett., 25*, 3759, 1998.

Shi, Y., and L. C. Lee, Structure of reconnection layer at the dayside magnetopause, *Planet. Space Sci., 38*, 437, 1990.

Sonnerup, B. U. O., and L. H. Cahill Jr., Explorer 12 observations of the magnetopause current layer, *J. Geophys. Res., 73*, 1757, 1968.

Sonnerup, B. U. O., Magnetic field reconnection, in *Solar System Plasma Physics*, Vol. III, edited by C. F. Kennel, L. J. Lanzerotti, and E. N. Parker, pp. 45-108, North-Holland, New York, 1979.

Sonnerup, B. U. O., G. Paschmann, I. Papamastorakis, N. Sckopke, G. Haerendel, S. J. Bame, J. R. Asbridge, J. T. Gosling, and C. T. Russell, Evidence for magnetic reconnection at the Earth's magnetopause, *J. Geophys. Res., 86*, 10,049, 1981.

Sonnerup, B. U. O., et al., The magnetopause for large magnetic shear: Analysis of convection electric fields from AMPTE/IRM, *J. Geophys. Res., 95*, 10,541, 1990.

Su, S.-Y., and B. U. O. Sonnerup, First-order orbit theory of rotational discontinuities, *Phys. Fluids, 11*, 851, 1968.

Swift, D. W., and L. C. Lee, Rotational discontinuities and the structure of the magnetopause, *J. Geophys. Res., 88*, 111, 1983.

Ugai, M., Self-consistent development of fast magnetic reconnection with anomalous plasma resistivity, *Plasma Phys. Controlled Fusion, 26*, 1549, 1984.

Yan, M., L. C. Lee, and E. R. Priest, Fast magnetic reconnection with small shock angles, *J. Geophys. Res., 97*, 8277, 1992.

H. Xie and Y. Lin, Physics Department, Auburn University, 206 Allison Laboratory, Auburn, AL 36849-5311. (hongx@physics.auburn.edu)

(Received April 13, 2000; revised July 10, 2000;
accepted July 24, 2000.)